Lattice Dynamics of EuO: Evidence for Giant Spin-Phonon Coupling

R. Pradip,[1,2] P. Piekarz,[3] A. Bosak,[4] D. G. Merkel,[4,*] O. Waller,[1,2] A. Seiler,[1,2] A. I. Chumakov,[4] R. Rüffer,[4] A. M. Oleś,[5,6] K. Parlinski,[3] M. Krisch,[4] T. Baumbach,[1,2,7] and S. Stankov[2,1,†]

[1]*Laboratory for Applications of Synchrotron Radiation, Karlsruhe Institute of Technology, D-76131 Karlsruhe, Germany*
[2]*Institute for Photon Science and Synchrotron Radiation, Karlsruhe Institute of Technology, D-76344 Eggenstein-Leopoldshafen, Germany*
[3]*Institute of Nuclear Physics, Polish Academy of Sciences, PL-31342 Kraków, Poland*
[4]*ESRF–The European Synchrotron, F-38000 Grenoble, France*
[5]*Max-Planck-Institut für Festkörperforschung, D-70569 Stuttgart, Germany*
[6]*Marian Smoluchowski Institute of Physics, Jagiellonian University, PL-30348 Kraków, Poland*
[7]*ANKA, Karlsruhe Institute of Technology, D-76344 Eggenstein-Leopoldshafen, Germany*

(Received 30 November 2015; published 2 May 2016)

Comprehensive studies of lattice dynamics in the ferromagnetic semiconductor EuO have been performed by a combination of inelastic x-ray scattering, nuclear inelastic scattering, and *ab initio* calculations. A remarkably large broadening of the transverse acoustic phonons was discovered at temperatures above and below the Curie temperature $T_C = 69$ K. This result indicates a surprisingly strong momentum-dependent spin-phonon coupling induced by the spin dynamics in EuO.

DOI: 10.1103/PhysRevLett.116.185501

Discovered in the early 1960s as the first rare-earth semiconducting oxide, EuO has remained an archetypal system for a Heisenberg ferromagnet (Curie temperature $T_C = 69$ K) until now. Initially known for its giant magneto-optic Kerr [1] and Faraday [2] effects, this fascinating oxide revealed a rich variety of other physical phenomena, such as metal-insulator transition with colossal magnetoresistance under doping [3], strain-induced manipulation of the T_C [4], and anomalous Hall effect [5]. Presently, it is one of the favored candidates for applications as a spin filter in future spintronic devices due to the large exchange splitting of its conduction band [6]. Indeed, EuO-based tunnel junctions have already demonstrated very high spin polarization efficiency [7] that, along with the recent integration on Si [8–10], classifies EuO as a potential workhorse in the Si-based spintronics.

It is surprising that the lattice dynamics of EuO, which is of fundamental importance for the proposed applications, is much less known, with only few early Raman studies [11,12]. Spin waves (magnons) in EuO and their linewidths ($\propto$ lifetime^{-1}) have been investigated in a broad temperature and momentum range [13–17]. Inelastic neutron scattering (INS) studies reported an anomaly in the spin-wave linewidth estimated from dynamical scaling arguments at T_C [15] and at larger wave vectors [16]. The spin-wave energy and linewidth dependence on the wave vector and temperature were studied within several theories [18–20], but the origin of the experimental linewidths and shapes remained to a certain extent unexplained. Other physical phenomena related to the lattice dynamics, such as a reduction of both the sound velocity [21] and thermal conductivity [22] at T_C, have been observed and attributed to spin-phonon coupling. Nevertheless, a direct experimental evidence for this coupling and its magnitude is still missing.

In this Letter we report the lattice dynamics study of EuO across its ferromagnetic transition employing modern synchrotron x-ray scattering techniques and first-principles calculations. We observed a large broadening of the transverse acoustic (TA) phonon branch along the Γ-X direction and a weak broadening of the longitudinal acoustic (LA) branch along the Γ-K-X direction slightly above and well below the Curie temperature. The obtained results uncover a remarkably strong and anisotropic spin-phonon interaction in EuO.

A 100 nm thick single crystalline EuO(001) film was grown on epipolished yttria stabilized zirconia YSZ(001) by reactive molecular beam epitaxy. Details on the sample growth and characterization are given in the Supplemental Material [23], see also Refs. [24–28]. Temperature-dependent momentum resolved spectra of inelastic x-ray scattering (IXS) were collected in grazing incidence geometry along Γ-X and Γ-K-X directions of the Brillouin zone at the beamline ID28 of the European Synchrotron (ESRF) using photons with an incident energy of 17.794 keV and an energy resolution of 3 meV [29]. The sample was measured under vacuum ($\approx 10^{-6}$ mbar) in a helium flow cryostat equipped with kapton foil windows for the x-ray beam. The phonon energies in Fig. 1 and linewidths were precisely determined by employing a model function consisting of a superposition of damped harmonic oscillator functions, convoluted with the predetermined resolution function, and numerically fitted to the IXS spectra [23]. Additionally, a temperature-dependent nuclear inelastic scattering (NIS) experiment on the EuO(001) film was performed at the Nuclear Resonance Beamline ID18 [30] of

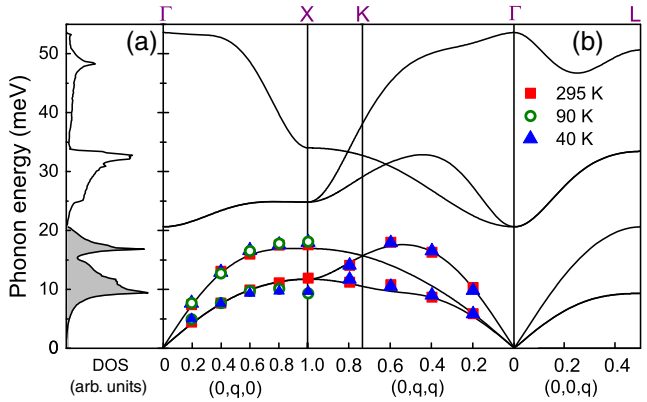

FIG. 1. (a) The *ab initio* calculated phonon DOS of EuO. The shaded area corresponds to the Eu-partial DOS. (b) Phonon dispersion relations from *ab initio* calculations (lines) and IXS experiments (points) at 295, 90, and 40 K.

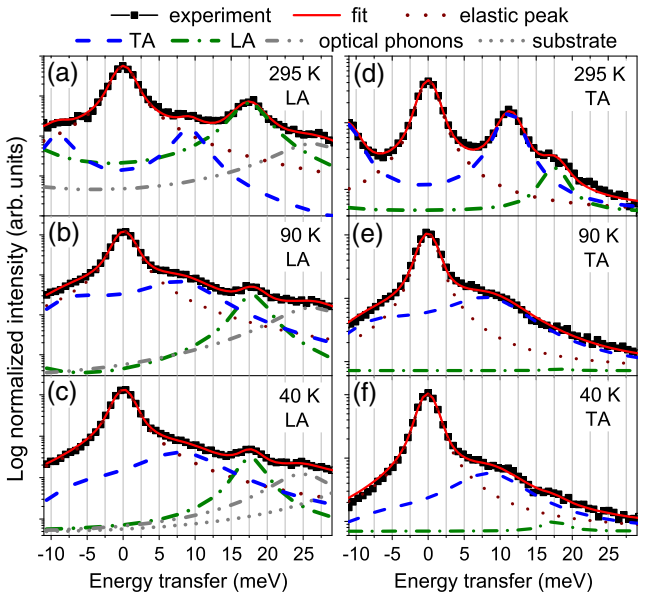

FIG. 2. Selected energy IXS scans for $q = 0.8$ along the Γ-X direction at the indicated temperatures. In (a)–(c) both the LA and TA phonons were excited, while in (d)–(f) mostly the TA excitations were probed. The complete data set and a detailed description of the fitting procedure are given in the Supplemental Material [23].

the ESRF to obtain the Eu-partial phonon DOS. The incident photon energy was tuned in the vicinity of the resonant transition energy (21.54 keV) of the ^{151}Eu nuclei with an energy resolution of 1.1 meV [31]. The sample was measured under vacuum ($\approx 10^{-6}$ mbar) in a helium flow cryostat equipped with kapton foil windows for the x-ray beam. The grazing incidence NIS data were collected with the wave vector of the incident photons parallel to the [010] direction of the EuO(001) film, corresponding to the Γ-X direction in the Brillouin zone. A standard procedure [32] was used to obtain the Eu-partial phonon DOS from the NIS spectra measured at several temperatures in the range 30–295 K.

Density functional theory was used to determine the lattice dynamics of EuO. The electronic structure was optimized within the projector augmented-wave method [33] and the generalized-gradient approximation (GGA) [34] implemented in the VASP software [35]. We have included a strong local Hubbard interaction ($U_f = 8.3$ eV, $U_p = 4.6$ eV) and Hund's exchange ($J_f = 0.77$ eV, $J_p = 1.2$ eV) [36] for the Eu($4f$) and O($2p$) states using the GGA + U method [37]. The optimized lattice parameter $a = 5.16$ Å corresponds well to the measured value 5.14 Å, and the calculated $4f$-$5d$ band gap of 1.05 eV agrees with the experimental value of 1.12 eV [38]. The phonon density of states and phonon dispersions (Fig. 1) were calculated using the direct method [39]. The Hellmann-Feynman forces were obtained by displacing nonequivalent atoms from their equilibrium positions to determine the force constants and dynamical matrices. Phonon energies and polarization vectors at a given wave vector follow from the exact diagonalization of the dynamical matrix.

Figure 1(b) reveals an excellent agreement between the experimental points obtained at the indicated temperatures and the *ab initio* calculated phonon dispersion relations. Compared to Eu metal [40], the energies of acoustic branches are increased by a few meV due to larger force constants in EuO. The weak scattering cross section of the oxygen atoms deterred us from tracing the optical branches at higher energies. The phonon energies remain fairly temperature independent, except an evident softening of the TA mode at low temperatures near the X point along the Γ-X direction ($\Delta E \approx 21\%$) that may arise from spin-phonon coupling.

Selected energy scans of IXS measured at a momentum transfer $q = 0.8$ along the Γ-X direction and at the indicated temperatures are shown in Fig. 2. Since the IXS intensity depends on the scattering vector and polarization of phonons, the scans plotted in Figs. 2(a)–2(c) and Figs. 2(d)–2(f) were measured in two different scattering geometries favoring the excitation of the LA and TA modes, respectively (for more details, see Supplemental Material [23]). At room temperature both the LA and TA peaks are well pronounced, exhibiting rather narrow linewidths. Reducing the temperature to 90 K leads to a drastic broadening of the TA mode, Figs. 2(d) and 2(e), while the width of the LA peak remains unaffected; see Figs. 2(a) and 2(b). The same phenomenon is observed for $T = 40$ K that is well below T_C; see Figs. 2(c) and 2(f).

The full widths at half maximum (FWHMs) derived from the fit to the experimental data [23] are plotted as functions of momentum transfer for the TA and LA branches along the Γ-X and Γ-K-X directions in Figs. 3(a) and 3(b) and Figs. 3(c) and 3(d), respectively. The FWHMs of the TA and LA modes along all the measured directions at room temperature remain weakly q

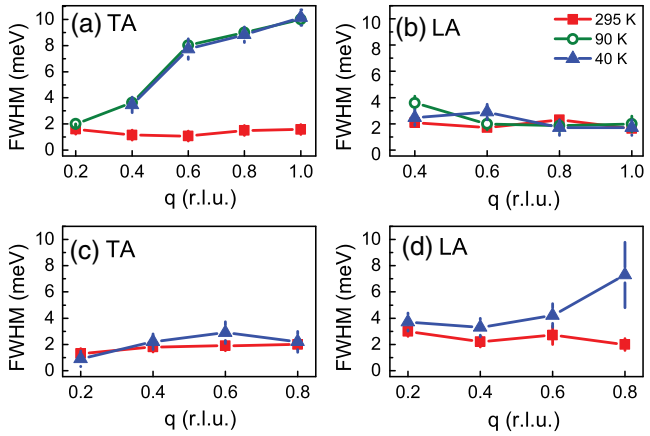

FIG. 3. (a),(b) FWHMs as a function of momentum transfer for the TA and LA branches along the Γ-X direction at 295, 90, and 40 K. (c),(d) FWHMs for the TA and LA branches along Γ-K-X direction at 295 and 40 K.

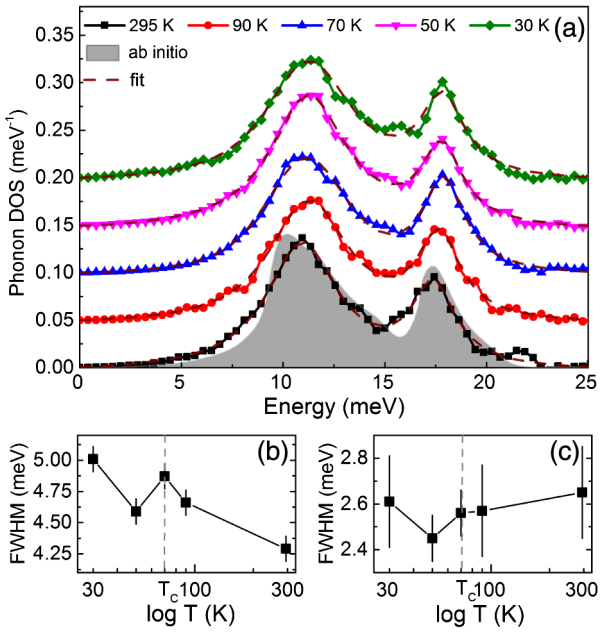

FIG. 4. (a) The Eu-partial phonon DOS in EuO obtained from the NIS experiment at the indicated temperatures. The spectra are up-shifted by 0.05 meV^{-1} for clarity. The *ab initio* calculated Eu-partial phonon DOS, convoluted with the instrumental resolution function, is depicted as shaded area. The dashed line stands for the fit of the experimental data with a combination of two Voigt profiles. The FWHM for increasing temperature for phonons at (b) 11 meV and (c) 17 meV. The solid lines are guides to the eye.

dependent throughout the entire Brillouin zone. We emphasize the remarkable q-dependent broadening of the TA modes along the Γ-X direction at $T = 90$ K and below; see Fig. 3(a). In fact, the phonon linewidth at the zone boundary increases by a factor of 5 from that measured at room temperature. Additionally, a weakly q-dependent broadening of the LA phonon modes along Γ-K-X is observed; see Fig. 3(d). In contrast to the Γ-X direction, the increase of the FWHMs for $q \leq 0.6$ is only a factor of 1.6 with respect to that measured at room temperature, with a clear tendency to increase towards the X point. At the same time, the widths of the LA and TA branches along Γ-X and Γ-K-X, respectively, remain temperature independent within the error bars; see Figs. 3(b) and 3(c).

Figure 4(a) shows the Eu-partial phonon DOS obtained at the indicated temperatures and reveals a good agreement with the *ab initio* calculated DOS convoluted with the instrumental function. A noticeable broadening of the TA peak at 11 meV with decreasing temperature is clearly visible. In order to estimate the width of the peaks at 11 and 17 meV, the DOS curves were approximated [dashed line in Fig. 4(a)] by a combination of two Voigt profiles. Figure 4(b) reveals an increase of the FWHMs of the TA modes with decreasing temperature, reaching about 17% at 30 K. The width of the second peak, which stems from the LA modes, however, is independent of temperature; see Fig. 4(c). These observations are in a qualitative agreement with the results from the IXS experiment. However, a direct quantitative comparison of the phonon linewidths obtained by IXS and NIS will be erroneous since the latter gives the momentum averaged and combined contributions from the LA and TA branches.

The observed phenomenon by both IXS and NIS experimental methods is surprising and in contrast to the usual decrease of phonon linewidths with decreasing T [41]. It demonstrates that a new type of coupling is activated by the spin dynamics. The inverse temperature dependence of the phonon broadening suggests that it is induced neither by scattering from defects nor by phonon-phonon interactions. In order to exclude anharmonic effects, the phonon energies were calculated assuming various atomic displacements, similarly to the previous studies on magnetite [42] (see also Supplemental Material [23]). The calculations show a negligible change in the phonon dispersions. The YSZ substrate with its matching crystal structure and lattice constant provides a strain-free template for the epitaxial growth of EuO films [23]. Consequently, anharmonicity and substrate-induced epitaxial strain are ruled out as the origin of the observed enormous increase of the TA phonon linewidths with decreasing T.

INS investigations of the spin dynamics in EuO have undoubtedly proven the presence of finite spin correlations above T_C up to 115 K [16,17,43]. Well-defined but heavily damped spin waves above T_C at the zone boundaries, mediated by exchange between nearest (NN) and next-nearest neighbor (NNN) Eu ions, have been experimentally observed [16,17] and theoretically confirmed [20], similar to Fe [44], Ni [45], and double perovskites [46]. The measured spin waves in EuO showed also an increasing linewidth towards the zone boundaries and were not accurately described most likely because their scattering from phonons was not considered. Following the Raman scattering experiments that reported a coupling of optical

phonons to spin waves [11,12], we attribute the observed increase of phonon linewidths towards the zone boundary at $T > T_C$ to an enhanced scattering of phonons by short-range spin excitations. Figure 3 reveals that phonon broadening is observed for the TA and LA modes along the Γ-X and Γ-K-X directions, in the ferromagnetic sample at 40 K. We recall the anomalous reduction of the sound velocity below T_C, which is believed to originate from strong coupling of spin fluctuations to acoustic phonons [21]. Thus, also for $T < T_C$, the spin-phonon coupling can be regarded as the mechanism behind the reduced phonon lifetimes obtained in our experiments.

A theoretical study of magnon-phonon coupling in a Heisenberg ferromagnet unveiled that the force constants acting between the NN and NNN play a decisive role in the spin-phonon coupling process [28]. Namely, for the TA modes the coupling is stronger towards the X point along Γ-X, while the LA modes couple more tightly to spin waves along Γ-K-X, provided that the force constants between the NNN are comparable to those acting between the NN. Our *ab initio* calculations indeed revealed that this condition is fulfilled for EuO (for details, see Supplemental Material [23]). In addition, the energies of the TA modes are closer to those of the spin waves (up to 6 meV [13]) compared to the LA modes. Even though the energies do not match exactly, they span a comparable range such that the momentum and energy conservation of the spin-phonon coupling process could be fulfilled. This explains the linewidth broadening observed in the TA modes along the Γ-X direction [Fig. 3(a)]. Contrary to the TA modes, the LA phonons show a pronounced broadening along the Γ-K-X direction [Fig. 3(d)]. We attribute this observation to the fact that these LA modes modulate the shortest Eu-Eu distance, thus affecting the magnetic exchange interaction between the localized $4f$ electrons. This effect is particularly strong at the zone boundary, where the NN atoms vibrate with opposite phases, which explains the increase of the phonon widths towards the X point.

Studies performed within the s-f model [47] revealed a large contribution of spin-phonon coupling to the phonon damping below and above T_C [48]. In order to estimate the spin-phonon coupling constant α, we use $\Gamma \approx \hbar\omega(zJ'^2/K)\chi_s''(\hbar\omega)$ [41], where Γ is the phonon width induced by spin fluctuations, $\hbar\omega$ is the phonon energy, z is the coordination number, J is the exchange coupling constant, K is the normalized force constant, and $J' = \alpha J/\text{Å}$ is the change of the exchange coupling constant J due to atomic displacement. We use $\chi_s''(\hbar\omega) \approx \hbar\omega(S/zJ)^2$ valid for a paramagnet. With $\Gamma \approx 8$ meV, $S = 7/2$, $z = 6$, $\hbar\omega = 10$ meV, and $K = 2.5$ eV/Å^2, we obtain $\alpha \approx 10$. This value is among the largest spin-phonon coupling constants observed [49,50]. Considering that the spin-phonon coupling in EuO arises from the Heisenberg and s-f exchange interactions and assuming a value of $\alpha_H \approx 4$ for the Heisenberg term [51], we deduce that $\alpha_{s\text{-}f} \approx 6$.

Furthermore, we have found an overall very good agreement in the temperature dependence of the Eu-projected vibrational entropy S_{vib} and lattice specific heat C_V of EuO, derived from the NIS experiment and the *ab initio* theory; see Supplemental Material [23]. However, we have detected neither an anomalous increase nor a critical behavior of the C_V at T_C. This is in agreement with the weak critical phonon scattering deduced from the thermal conductivity [52] and implies that the anomaly observed by calorimetric experiments [53,54] is not connected with the lattice excitations, but it arises from the magnetic contribution to the specific heat [55]. The normalized mean force constant K remains unchanged within the error bars for the entire temperature range that is consistent with the weak anharmonicity in EuO.

In conclusion, we have determined the lattice dynamics of EuO in a broad temperature range across the T_C by IXS, NIS, and first-principles calculations. The experiments unambiguously reveal a remarkable broadening of the phonons at low temperatures, especially pronounced for the TA modes along the Γ-X direction. This is unexpected and implies a surprisingly strong spin-phonon coupling activated by spin fluctuations, which influences the electronic states and the lattice dynamics. The large spin-phonon coupling reported here seems to be the missing component for the accurate interpretation of the spin-wave linewidth dependence on temperature and momentum obtained by INS experiments [15,16,20]. Moreover, such noticeable anisotropic coupling is of relevance for the proposed application of EuO in spintronics. Our results show that the magnitude of the spin-phonon coupling in EuO is smaller along the Γ-K-X than along the Γ-X direction, implying that the choice of crystal orientation could be crucial for reducing the undesired spin flips.

We thank Giniyat Khaliullin and Paweł T. Jochym for valuable discussions. We are grateful to B. Krause, A. Weißhardt, and H. H. Gräfe for the support in the UHV-Analysis Lab. We acknowledge ESRF–The European Synchrotron for provision of synchrotron radiation facilities, the Materials Preparation Center at Ames Laboratory, which is supported by the U.S. DOE Basic Energy Sciences, for providing the Eu source material, and the Excellence Initiative for the financial support of the UHV-Analysis Lab via the project KIT-Nanolab@ANKA. S. S. acknowledges the financial support by the Initiative and Networking funds of the President of the Helmholtz Association and the Karlsruhe Institute of Technology (KIT) for the Helmholtz-University Young Investigators Group "Interplay between structure and dynamics in epitaxial rare earth nanostructures" Contract No. VH-NG-625. P. P. and A. M. O. kindly acknowledge support by Narodowe Centrum Nauki (NCN) under Projects No. 2011/01/M/ST3/00738 and No. 2012/04/A/ST3/00331.

*On leave from Institute for Particle and Nuclear Physics, Wigner Research Centre for Physics, Hungarian Academy of Sciences, H-1525 Budapest, Hungary.
†Corresponding author.
Svetoslav.Stankov@kit.edu

[1] J. H. Greiner and G. J. Fan, Appl. Phys. Lett. **9**, 27 (1966).
[2] K. Y. Ahn, J. Appl. Phys. **41**, 1260 (1970).
[3] Y. Shapira, S. Foner, and R. Aggarwal, Phys. Rev. B **8**, 2316 (1973).
[4] A. Melville, T. Mairoser, A. Schmehl, T. Birol, T. Heeg, B. Holländer, J. Schubert, C. J. Fennie, and D. G. Schlom, Appl. Phys. Lett. **102**, 062404 (2013).
[5] T. Yamasaki, K. Ueno, A. Tsukazaki, T. Fukumura, and M. Kawasaki, Appl. Phys. Lett. **98**, 082116 (2011).
[6] P. G. Steeneken, L. H. Tjeng, I. Elfimov, G. A. Sawatzky, G. Ghiringhelli, N. B. Brookes, and D. J. Huang, Phys. Rev. Lett. **88**, 047201 (2002).
[7] T. S. Santos, J. S. Moodera, K. V. Raman, E. Negusse, J. Holroyd, J. Dvorak, M. Liberati, Y. U. Idzerda, and E. Arenholz, Phys. Rev. Lett. **101**, 147201 (2008).
[8] A. Schmehl *et al.*, Nat. Mater. **6**, 882 (2007).
[9] R. P. Panguluri, T. S. Santos, E. Negusse, J. Dvorak, Y. Idzerda, J. S. Moodera, and B. Nadgorny, Phys. Rev. B **78**, 125307 (2008).
[10] C. Caspers, M. Müller, A. X. Gray, A. M. Kaiser, A. Gloskovskii, C. S. Fadley, W. Drube, and C. M. Schneider, Phys. Rev. B **84**, 205217 (2011).
[11] J. C. Tsang, M. S. Dresselhaus, R. L. Aggarwal, and T. B. Reed, Phys. Rev. B **9**, 984 (1974).
[12] P. Grünberg, G. Güntherodt, A. Frey, and W. Kress, Physica B (Amsterdam) **89**, 225 (1977); G. Güntherodt, R. Merlin, and W. Grünberg, Phys. Rev. B **20**, 2834 (1979); R. Zeyher and W. Kress, Phys. Rev. B **20**, 2850 (1979).
[13] L. Passell, O. W. Dietrich, and J. Als-Nielsen, Phys. Rev. B **14**, 4897 (1976).
[14] J. Als-Nielsen, O. W. Dietrich, and L. Passell, Phys. Rev. B **14**, 4908 (1976).
[15] O. W. Dietrich, J. Als-Nielsen, and L. Passell, Phys. Rev. B **14**, 4923 (1976).
[16] H. A. Mook, Phys. Rev. Lett. **46**, 508 (1981).
[17] P. Böni and G. Shirane, Phys. Rev. B **33**, 3012 (1986).
[18] V. Vaks, A. Larkin, and S. Pikin, Sov. Phys. JETP **26**, 188 (1968).
[19] R. Raghavan and D. L. Huber, Phys. Rev. B **14**, 1185 (1976).
[20] A. P. Young and B. S. Shastry, J. Phys. C **15**, 4547 (1982).
[21] B. Lüthi and R. J. Pollina, Phys. Rev. Lett. **22**, 717 (1969).
[22] R. G. Morris and J. L. Cason, Helv. Phys. Acta **41**, 1045 (1968).
[23] See Supplemental Material at http://link.aps.org/supplemental/10.1103/PhysRevLett.116.185501, for sample preparation and characterization, evaluation of inelastic x-ray scattering data, *ab initio* calculations and thermoelastic properties.
[24] R. Sutarto *et al.*, Phys. Rev. B **79**, 205318 (2009).
[25] R. W. Ulbricht, A. Schmehl, T. Heeg, J. Schubert, and D. G. Schlom, Appl. Phys. Lett. **93**, 102105 (2008).
[26] M. A. Andreeva, Hyperfine Interact. **185**, 17 (2008).
[27] H. H. Wickman, J. Appl. Phys. **39**, 1248 (1968).
[28] T. M. Cheng and L. Li, J. Magn. Magn. Mater. **320**, 1 (2008).
[29] M. Krisch and F. Sette, *Light Scattering in Solid IX*, edited by M. Cardona and R. Merlin, Topics in Applied Physics Vol. 108 (Springer, Berlin, 2007), pp. 317–370.
[30] R. Rüffer and A. I. Chumakov, Hyperfine Interact. **97–98**, 589 (1996).
[31] O. Leupold, J. Pollmann, E. Gerdau, H. D. Rüter, G. Faigel, M. Tegze, G. Bortel, R. Rüffer, A. I. Chumakov, and A. Q. R. Baron, Europhys. Lett. **35**, 671 (1996).
[32] V. Kohn and A. I Chumakov, Hyperfine Interact. **125**, 205 (2000).
[33] P. E. Blöchl, Phys. Rev. B **50**, 17953 (1994).
[34] J. P. Perdew, K. Burke, and M. Ernzerhof, Phys. Rev. Lett. **77**, 3865 (1996).
[35] G. Kresse and J. Furthmüller, Comput. Mater. Sci. **6**, 15 (1996).
[36] N. J. C. Ingle and I. S. Elfimov, Phys. Rev. B **77**, 121202 (2008).
[37] V. I. Anisimov, J. Zaanen, and O. K. Andersen, Phys. Rev. B **44**, 943 (1991).
[38] G. Busch, G. Güntherodt, and P. Wachter, J. Phys. (Paris), Colloq. **32**, 928 (1971).
[39] K. Parlinski, Z-. Q. Li, and Y. Kawazoe, Phys. Rev. Lett. **78**, 4063 (1997).
[40] S. Stankov, P. Piekarz, A. M. Oleś, K. Parlinski, and R. Rüffer, Phys. Rev. B **78**, 180301 (2008).
[41] C. Ulrich, G. Khaliullin, M. Guennou, H. Roth, T. Lorenz, and B. Keimer, Phys. Rev. Lett. **115**, 156403 (2015).
[42] M. Hoesch, P. Piekarz, A. Bosak, M. Le Tacon, M. Krisch, A. Kozłowski, A. M. Oleś, and K. Parlinski, Phys. Rev. Lett. **110**, 207204 (2013).
[43] R. Chaudhury and B. S. Shastry, Phys. Rev. B **37**, 5216 (1988).
[44] X. Tao, D. P. Landau, T. C. Schulthess, and G. M. Stocks, Phys. Rev. Lett. **95**, 087207 (2005).
[45] V. Antropov, Phys. Rev. B **72**, 140406(R) (2005).
[46] S. M. Zhou, Y. Q. Guo, J. Y. Zhao, S. Y. Zhao, and L. Shi, Appl. Phys. Lett. **96**, 262507 (2010).
[47] W. Nolting and A. M. Oleś, Phys. Rev. B **22**, 6184 (1980); **23**, 4122 (1981).
[48] J. M. Wesselinowa and A. T. Apostolov, J. Phys. Condens. Matter **5**, 3555 (1993).
[49] B. Normand, H. Kohno, and H. Fukuyama, Phys. Rev. B **53**, 856 (1996).
[50] R. Werner, C. Gros, and M. Braden, Phys. Rev. B **59**, 14356 (1999).
[51] W. Baltensperger and J. S. Helman, Helv. Phys. Acta **41**, 668 (1968).
[52] J. J. Martin and G. S. Dixon, Phys. Status Solidi B **54**, 707 (1972).
[53] A. Kornblit and G. Ahlers, Phys. Rev. B **11**, 2678 (1975).
[54] K. Ahn, A. O. Pecharsky, K. A. Gschneidner, and V. K. Pecharsky, J. Appl. Phys. **97**, 063901 (2005).
[55] B. E. Argyle, N. Miyata, and T. D. Schultz, Phys. Rev. **160**, 413 (1967).